

Assessing the Wave Energy Resource Using Remote Sensed Data

M. T. Pontes¹, M. Bruck^{1,2}, S. Lehner²

1- LNEG, Laboratório Nacional de Energia e Geologia
Estrada do Paço do Lumiar, 1649-038 Lisboa, Portugal
E-mail: teresa.pontes@lneg.pt

2- DLR- German Aerospace Centre
Oberpfaffenhofen, Münchner Straße 20 82234 Weßling Germany
E-mail: Miguel.Bruck@dlr.de
E-mail: Susanne.Lehner@dlr.de

Abstract

The use of accurate remote sensed wave data in the coastal area (water depth up to 80m) will enable a high quality characterization of the wave energy resource. Work has been carried out with this objective for a number of years namely assessing the quality of the radar altimeter and SAR sensors data.

In this paper a summary of the quality of wave period estimates from the NASA/CNES Jason radar altimeter is presented, showing that the analytical models that have been proposed in recent years provide already accurate results.

This paper also includes a verification of ESA ENVISAT SAR data (height, period and direction parameters in addition to the shape of frequency spectra) against NDBC buoy data, which has shown good accuracy for wave energy resource assessment. However, the long Exact-Repeat-Period of NASA (10 days) and of ESA satellites (35 days) poses serious limitation to the usefulness of their wave measurements except for long-term wave climate assessment. These shortcomings are expected to be overcome by the new high spatial-resolution TerraSAR-X satellite that is obtaining reliable data for nearshore areas, being able to provide data at 2 - 3 day interval.

Keywords: Remote Sensed (altimeter and SAR) Data, Period Algorithms, Directional Spectra.

Nomenclature

CERSAT = Centre ERS d'Archivage et de Traitement (IFREMER)
CNES = Centre National d'Études Spatiales
CSA = Canadian Space Agency

DLR = German Aerospace Centre
DWD = German Meteorological Office
ECMWF = European Centre Medium Range Weather Forecast
ERS = European Remote Sensing Satellite
ESA = European Space Agency
NOAA = National Oceanic and Atmospheric Administration
NASA = National Aeronautics and Space Administration
NDBC = National Data Buoy Centre
SAR (ASAR) = (Advanced) Synthetic Aperture Radar
WERATLAS = European Wave Energy Atlas

1. Introduction

The assessment of the wave energy resource has been mostly carried out based on results of wind-wave models that, at low cost, produce accurate results over large or small areas of the ocean. These numerical models solve the wave energy balance equation at the nodes of a grid covering the ocean (from global to local scales) producing directional spectra $S(f, \theta)$ that describe the distribution of energy density in frequency and direction domains, or in wave number space. From such spectra wave height, period and direction parameters are computed which constitute a useful description of the basic characteristics of sea states. The accuracy of wind-wave models has continued to increase in the last decade due to a better description of the physics of ocean waves as well as due to data assimilation, namely buoy data and remote sensed data. One should mention the usefulness for this application of the Global Telecommunication System (GTS) that carries out various types of meteorological data (<http://www.wmo.int/pages/prog/www/TEM/XGTS/gts.html>).

In addition to being used in data assimilation (e.g. in the WAM model that is in the routine operation of the ECMWF and the Wave Watch III, at NOAA), or for specific purposes (e.g. in the development of WERATLAS - European Wave Energy Atlas, Pontes

[1]), remote sensed wave data have been tested for direct use in wave energy resource studies.

Imaging radar is an active illumination system, in contrast to passive imaging systems that require Sun's illumination. Radar uses a single frequency for illumination; therefore there is no colour associated with raw radar imagery but it provides at least two significant benefits: the ability to image through clouds and to image day and night. These systems emit a pulse of electromagnetic microwaves whose backscatter off the surface is received by the antenna that emitted the pulse. To measure ocean waves two types of space-borne radars are used. These are the altimeter and the Synthetic Aperture Radar (SAR).

Table 1 shows that the distance between satellite tracks in the Equator varies from about 80 km for the ESA satellites to more than 300 km for NASA/CNES satellites (Jason's and the preceding Topex/Poseidon), while the Exact Repeat Period (time interval between two successive passages over a location) decreases from 35- to about 10-day. It is then clear that to obtain a permanent coverage of the whole globe a constellation of various satellites is needed.

The first source of satellite-based wave data has been the radar altimeter that is based on the measurement of the backscatter of the pulse emitted by its antenna; it provides significant wave height H_s , wind speed at 10m height U_{10} in addition to the backscatter coefficient σ_0 . The accuracy of significant wave height obtained from altimeter is high being comparable to that of wave buoy data.

However for wave energy conversion the knowledge of wave period is also essential. Several analytical models that compute zero-crossing period T_z from altimeter data started to be proposed more than ten years ago.

| Satellite | Start | Agency | Dual Band | GTS-E (km) | ERP (day) |
|--------------------------|--------------|---------------|-----------|------------|-----------|
| ERS-2 | 1995 | ESA | No | 78 | 35 |
| Radarsat 1 Radarsat 2 | 1995 2007 | CSA | No | | |
| GFO | 1998 | US Navy | No | - | 17 |
| Jason 1 Jason 2 | 2001 2008 | NASA/ CNES | Yes | 315 | 9.9 |
| ENVISAT | 2002 | ESA | Yes | 80 | 35 |
| TerraSAR-X | 2007 | DLR | No | - | 11 |

Table 1: Main features of Earth Observation Satellites. GTS-E – Equator ground track separation, ERP – Exact Repeat Period. See [2] for RadarSat

Section 2 summarizes the quality of the various models showing that T_z estimates from altimeter data are already accurate, enabling in this way to consider satellite altimeters as a reliable source of useful non-directional data for wave energy resource assessment.

From the Synthetic Aperture Radar (SAR) estimates of directional wave spectra $S(f, \theta)$ are obtained. However up to now the ASAR wave spectra that are distributed by the European Space Agency (ESA) are considered to be correct only for low frequency waves (generally longer than 140m) therefore their use for wave energy resource assessment in areas where wind-waves dominate (e.g. North Sea) should be limited.

Recently (2007) TerraSAR-X (TSX) satellite was launched. It will enable obtaining more detailed information namely in the nearshore/coastal area. Section 3 includes an overview and analysis of SAR data. A comparison between ENVISAT ASAR and US NDBC buoy wave data is presented, including verification of sea-state parameters as well as energy density spectral shape whose accuracy is relevant for the design of wave energy converters.

Finally, conclusions and plans for further work are summarized in Section 4.

2. Satellite Altimetry

Since 1991 at least one satellite altimeter has been in operation. This was started by ESA ERS-1 satellite that was followed in 1992 by the NASA/CNES TOPEX/Poseidon (T/P). ESA ERS-1 was followed by ERS-2 in 1996; ENVISAT was launched in 2002. (It should be noted that all the ESA satellites carry SAR sensors). The US Navy launched Geosat Follow-on (GFO) in 2000 and in 2001 NASA/CNES replaced T/P by Jason, and Jason 2 was launched in 2008. Presently eight radars are measuring ocean waves from space their main characteristics being presented in Table 1.

The first useful analytical models that enable computing wave period from altimeter data were proposed by Davies et al. [3]; this was followed by a simpler algorithm by Gommenginger et al. [4] which was updated by Caires et al. [5]. Using a different approach, Quilfen et al. [6] developed a neural-network set of two algorithms. Such models compute zero-crossing period T_z from altimeter H_s , U_{10} and σ_0 data. The first one uses only altimeter Ku-band data while the second one uses also C-band data.

Quilfen Model 1

$$T_z = \exp(-17.1642A + 13.5844) \quad (1)$$

where A is defined by

$$A = \frac{1}{1 + \exp(0.6573H_s^{0.1084} \sigma_{Ku}^{0.2962} - 2.2377)} \quad (2)$$

Quilfen Model 2

$$T_z = \exp(5.7474 - 1.4688B) + 1.7943C \quad (3)$$

where B and C are given by

$$B = \frac{\sigma_{Ku}^{0.3082}}{\sigma_C^{0.2352} H_s^{0.0981}} \exp(1.5068C) \quad (4)$$

$$C = \frac{2}{1 + \exp(-1.8612 - 0.08U_{10})} - 1 \quad (5)$$

In Pontes and Bruck [7] a comparison of four models that compute T_z from altimeter data is presented, which is summarized in Table 2.

| Model | R^2 | Bias | E_a | E_{rms} | S_i |
|--------------|-------|-------|-------|-----------|-------|
| Davies | 0.79 | 0.09 | 0.54 | 0.72 | 0.11 |
| Gommenginger | 0.72 | 0.08 | 0.60 | 0.77 | 0.12 |
| Quilfen 1 | 0.87 | 0.14 | 0.41 | 0.54 | 0.08 |
| Quilfen 2 | 0.89 | -0.02 | 0.33 | 0.46 | 0.07 |

Table 2: Comparison of T_z model estimates from Jason altimeter data against NDBC buoy data.

Table 2 shows the error statistics obtained from the comparison of Jason T_z data computed by the various models referred to above against NDBC buoy data. The statistics include bias, absolute error E_a , root-mean square error E_{rms} and scatter index S_i (ratio of E_{rms} and buoy mean value), in addition to the determination coefficient R^2 (R being the correlation coefficient). These comparisons show that the agreement is good, with bias generally smaller than 1s, S_i varying between 7% and 12% and R being larger than 0.85.

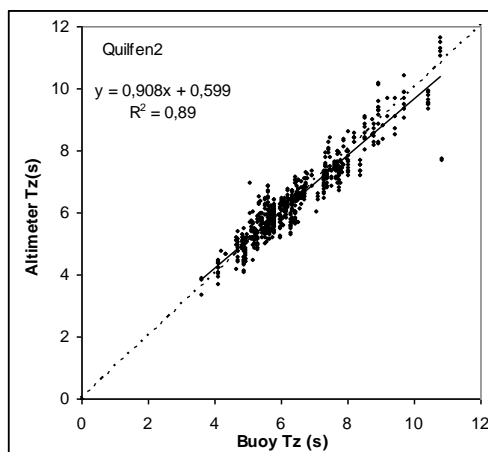


Fig. 1: Comparison of T_z computed from Quilfen et al. model 2 [5] from Jason altimeter data against NDBC collocated buoys data. The solid line is the regression line (equation in the box). Number of pairs of observations Nobs = 640.

This comparison shows that it is the neural-network Quilfen et al. model 2 [6] that presents the best (and

good) accuracy. This verification was made using collocated Jason altimeter and USA NDBC buoys data with 36 km maximum space separation and 30 min maximum time difference. This joint dataset was processed and is available at CERSAT <http://www.ifremer.fr/cersat/en/index.htm>. It includes 640 pairs of altimeter-buoy quality-checked data measurements during the period July-December 2005. Figure 1 presents the scatter diagram of the 640 pairs of collocated T_z computed from Jason using Quilfen et al. model 2 and buoy data.

3. Satellite Synthetic Aperture Radar

The synthetic aperture radar (SAR) yields high resolution two dimensional images of the radar backscatter properties of the sea surface and is thus used to measure wind fields and sea state from space. The use of Synthetic Aperture Radars on board of satellites was started in the 1990s by the European Space Agency (ESA) in its ERS's satellites, which were followed by ENVISAT in 2002. Estimates of directional spectra are being obtained from the ENVISAT Advanced Synthetic Aperture Radar (ASAR) product Wave Mode Level 2. This product corresponds basically to measurements in small *wave cells* (circa 5km - 10 km length) that are acquired at 100 km intervals. The spectra are provided in wave-number space (wavelength 800 m to 30 m) that in deep-water correspond to $0.044 < f < 0.2288$ Hz (period between 22.7 and 4.4s).

3.1 ENVISAT ASAR

In order to assess the usefulness of ENVISAT ASAR wave information for wave energy resource studies, a comparison was made of significant wave height H_s , energy (mean) period T_e , zero-crossing period T_z , peak period T_p , and wave power (flux of energy per unit crest length) P to the corresponding ones obtained from USA NDBC collocated buoy data. ASAR spectral frequency shapes ($E(f) = \int S(f, \theta) d\theta$) were also compared to those obtained from NDBC buoy measurements. In the open ocean areas (including the western coasts of Europe and United States where the highest wave energy resource can be found) swells provide the most important contribution for the available wave power. It is therefore important that the accelerometer of the wave measuring buoys whose data will be used for ASAR products validation provides high resolution in the low-frequency range. Only two of the NDBC buoys in operation on 2005-2006 possess such an accelerometer (Datowell Hippy 40 accelerometer, see e.g. <http://download.datowell.nl/>).

To assess the accuracy of the ENVISAT ASAR spectral information, a detailed comparison of the wave parameters referred to above obtained from ASAR directional spectra and from NDBC 51001 and 51028 buoy data in 2005-2006 was made. Only pairs of data with small spatial distances (less than 36 km) and short time difference (up to 30 min) were considered. Buoy

51001 is located at 23° 26'42" N 162° 16'43" W (NW of Kauai island, Hawaii) at 3252 m water-depth and buoy 51028 at 0° 0' 4" N 153° 54'46" W, water-depth of 4747m. It should be noticed that only a small number of collocated ASAR and buoy data pairs were found (14 for buoy 51001 and 11 for buoy 51028) but the accuracy for each pair of data is similar.

Wave and Power Parameters

Tables 3 and 4 present the error statistics of ASAR-spectra derived wave and power parameters.

| | H_s (m) | T_e (s) | T_z (s) | P (kW/m) |
|-----------|-----------|-----------|-----------|------------|
| R^2 | 0.76 | 0.74 | 0.51 | 0.63 |
| Bias | -0.06 | 0.58 | 0.31 | -1.57 |
| E_{rms} | 0.14 | 0.69 | 0.47 | 3.56 |
| S_i | 0.07 | 0.08 | 0.06 | 0.17 |

Table 3: Verification of wave parameters obtained from ENVISATASAR spectra against NDBC buoy 51028 (Equator). Data for 2005-2006. Nobs = 11.

| | H_s (m) | T_e (s) | T_z (s) | P (kW/m) |
|-----------|-----------|-----------|-----------|------------|
| R^2 | 0.77 | 0.69 | 0.81 | 0.73 |
| Bias | 0.07 | 0.63 | 0.45 | 1.19 |
| E_{rms} | 0.36 | 0.93 | 0.85 | 6.13 |
| S_i | 0.18 | 0.11 | 0.11 | 0.34 |

Table 4: Same as Table 3 for buoy 51001 (NW of Kauai Island, Hawaii). Nobs=14.

These tables show that the accuracy for the ASAR at the Equator location (buoy 51028) is quite good, with H_s scatter index $S_i = 7\%$, and S_i being 8 and 7% for energy period and zero-crossing period, and 11% for wave power; the correlation coefficient R varies between 0.83 and 0.9.

For the Hawaii area (buoy 51028), the error statistics present slightly higher values for all wave parameters considered, namely $S_i = 18\%$ for H_s , S_i is 11% for the two period parameters and is 34% for power. The correlation coefficient R is slightly lower than for the Equator (buoy 51028 buoy) varying between 0.71 for T_z and 0.87 for H_s .

Spectral Shape

For wave energy conversion it is also important to assess the accuracy of the spectral shape $E(f)$ in order to maximize the conversion efficiency of wave energy converters; these converters should be designed for maximum conversion efficiency at the peak frequency band (with highest energy content).

In this context it should be taken into account that ESA warns that the ENVISAT ASAR provides reliable spectral information only for frequencies lower than the cut-off frequency f_{cut} . Because wave spectra are derived from a radar image, f_{cut} depends on the waves orbital velocity thus it varies with wave conditions. In this

study, $0.07 < f_{cut} < 0.11$ Hz, i.e. the corresponding cut-off period) lies between 14.3 and 9.1s.

Figures 2 to 5 present spectral shape comparison for buoys 51001 and 51028 against the corresponding buoy spectra. Sea-states with power ranging from less than 10 kW/m (low energy) to almost 40 kW/m (average energy) where selected.

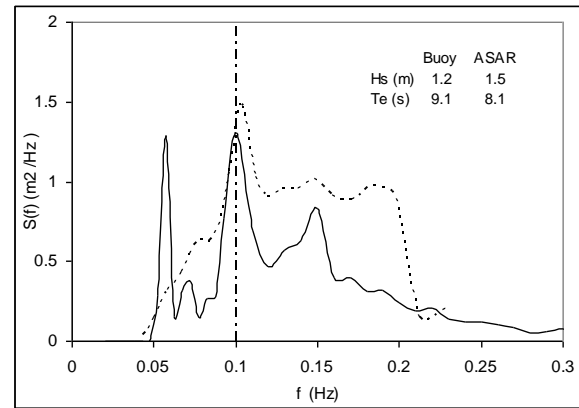


Fig. 2: Comparison of buoy 51001 (solid line) and ASAR (dashed line) $E(f)$ on 2006.09.14. Vertical line (dashed) represents f_{cut} . Spatial distance between two measurement spots is $dx = 28$ km, time elapsed $dt = 12$ min, $P = 6.4$ kW/m (buoy) and $P = 8.9$ kW/m (ASAR).

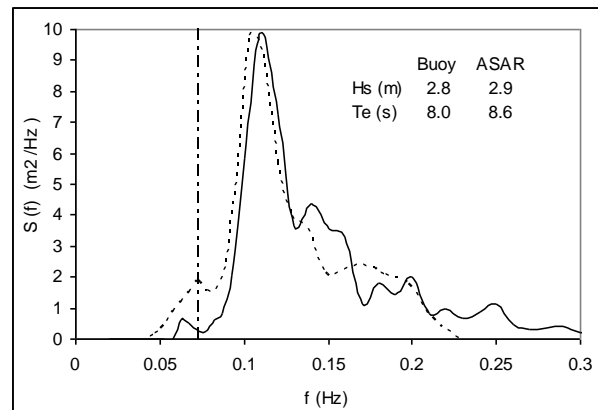


Fig. 3: Same as Fig.2 on 2006.04.17. $dx = 34$ km, $dt = 19$ min, $P = 30$ kW/m (buoy) and $P = 35$ kW/m (ASAR).

Except in Fig. 2 (low-energy sea-state) when the buoy identified a long low-energy swell but ASAR did not, a general fair agreement between the $E(f)$ shape was obtained from ASAR and buoy measurements, namely they coincided in the presence of wind-sea and swell systems and their frequency range. One should notice that the agreement is good as expected for the low frequency band ($f < f_{cut}$) as well as for the higher frequency band ($f > f_{cut}$) where the ENVISAT ASAR frequency spectrum is not considered to be reliable. Further tests need to be realized, taking in consideration the relationship between the direction of wave propagation and the satellite track, in order getting more

confidence that enables using such data for design of wave energy converters.

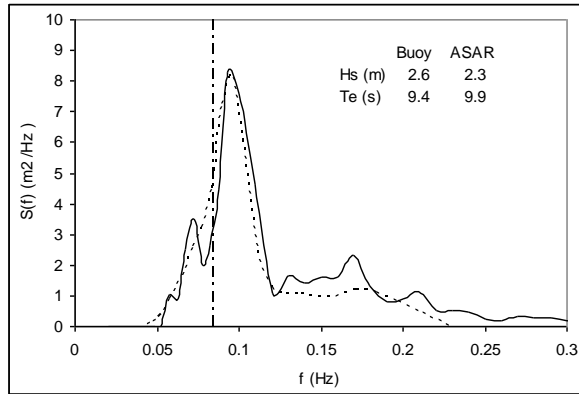


Fig. 4: Comparison of ASAR and buoy 51028 $S(f)$ on 2006.01.15. $dx = 34$ km, $dt = 25$ min. $P = 31.2$ kW/m (buoy) and $P = 25.7$ kW/m (ASAR).

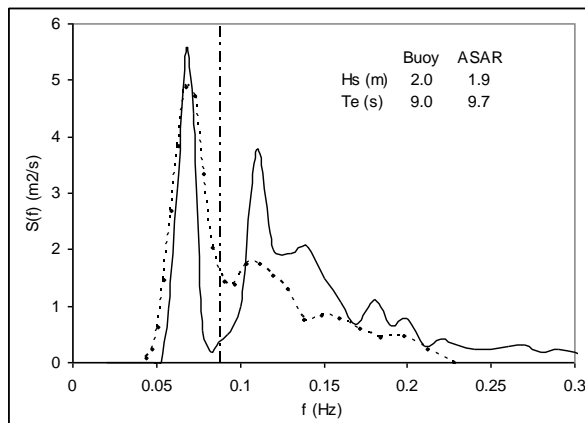


Fig. 5: Same as Fig. 4 on 2006.09.17. $dx = 30$ km, $dt = 25$ min. $P = 17.7$ kW/m (buoy) and $P = 17.2$ kW/m (ASAR).

3.2 TERRASAR-X

In June 2007 the German Aerospace Centre (DLR) jointly with Infoterra GmbH launched the TerraSAR-X (TSX) satellite that is a high resolution right looking radar; its images are accessible to scientific users since December 2007. TSX carries a high frequency X-band SAR sensor that can be operated in different modes (coverage and resolution). Due to its polarimetric and interferometric capabilities as well as the high spatial resolution of up to 1m, the TerraSAR-X sensor is a very interesting tool for coastal oceanography.

The TSX sensor operates for scientific use in the following modes:

- the "Spotlight" mode with 10 x 10 km scenes at a resolution of 1-2 meters,
- the "Stripmap" mode with 30 km wide strips at a resolution between 3 and 6 meters,

- the "ScanSAR" mode with 100 km wide strips at a resolution of 16 meters.

For coastal applications TSX is often used in stripmap mode, in order to achieve better coverage at still a high resolution of 3 meters.

Figure 6 shows the effect of the achieved higher resolution comparing images of ENVISAT with a pixel size of 12 meters to a TSX stripmap image. The images were acquired over the German island of Norderney showing a 2 km by 7 km subscene.

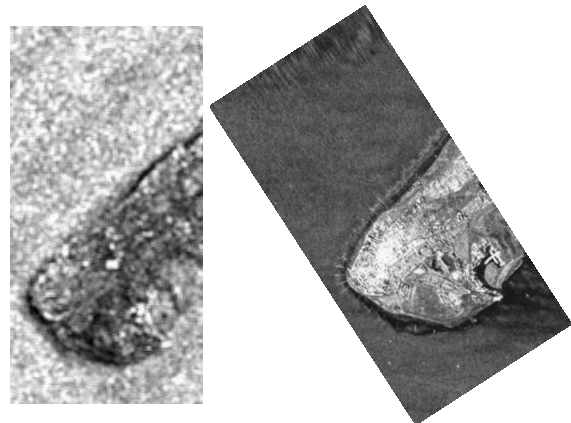


Fig. 6: ENVISAT image mode SAR image (left) on April 2004, (right) TSX stripmap acquired on August 27, 2007.

Over the sea surface, TerraSAR X Radar images are used for measurement of the wind field and the sea state. On what regards ocean surface waves in the coastal area, these images enable to observe shoaling waves, changing wave length and direction and finally breaking on the sand bars. From the radar images significant wave height, wave length and direction are already determined. Ocean waves can be observed with a peak wave length from approximately 15 meters as compared to only 100 to 150 meters for ERS and ENVISAT. Therefore it is possible to measure sea states now in areas in which ocean waves were too short in wave length to be detectable by the conventional radar satellites as, e.g., the Baltic Sea, and large lakes.

A comparison of TSX H_s , T_e , T_z and T_p and mean direction- derived values against results of the DWD wind-wave model WAM model has started; the preliminary results have shown good agreement. It is expected to obtain more confidence on these data within a several months period of time .

4. Conclusions and Plans

In this review, it was found that radar altimeters became a useful source of wave data for preliminary wave energy resource studies because accurate significant wave height data are obtained from the sensor measurements and analytical models have been

developed that compute accurately zero-crossing period. However, these sensors provide no directional information, which is essential when non-axysymmetrical converters are being considered.

From the Synthetic Aperture Radar (SAR) directional spectra are obtained but their accuracy for high frequency band is not ensured by ESA for the ENVISAT ASAR wave mode product. However a comparison of spectral shape in various sea-sates showed good fitting of ASAR $E(f)$ against NDBC buoy data. It is then advisable to pursue this comparison taking into account the relationship between satellite tracking direction and wave propagation direction. It is also planned to verify the accuracy of the ASAR spectral directional distribution through the comparison against buoy data.

Finally, the new high spatial resolution TerraSAR-X sensor was presented that enables the measurement of wind and waves in the coastal area. The undergoing work to obtain reliable wave information is expected to enable in the near future the use of TSX wave data in nearshore areas.

Acknowledgments

Part of the work presented in this paper was developed within the Portuguese FCT Contract N° PDCT/MAR/61463/2004. The collocated Jason/NDBC buoy data set was provided by IFREMER within a visit by M. Bruck, which was supported by EC FP6 Contract *Co-ordination Action on Ocean Energy*.

The ENVISAT ASAR data were provided by ESA within the Category 1 Proposal N° 3936 “Advanced Ocean Surface Data: Wave Energy Utilization and Primary Production”. Buoy data were retrieved from NOAA’s National Data Buoy Centre archives.

References

- [1] Pontes, M.T., Assessing the European Wave Energy Resource. *Transactions of ASME: Journal of Offshore Mechanics and Arctic Engineering*, vol. 120, pp. 226-231, 1998.
- [2] Luscombe, A.P. et al; "The RADARSAT Synthetic Aperture Radar Development", *Canadian Journal of Remote Sensing*, Volume 19, No. 4, Nov-Dec 1993, p. 302.
- [3] Davies, C.G., P. D. Cotton, P. G. Challenor and D.J. Carter. On the Measurements of Wave Period from Radar Altimeters, Ocean Wave Measurements and Analysis. *Proc. 3rd Int. Symp. Waves '97*, ASCE, Reston, VA, 819-826, 1998.
- [4] Gommenginger, C. P., M.A. Sroksoz, P. G. Challenor. Measuring ocean wave period with satellite altimeters: A simple empirical model. *Geophysical Research Letters*, vol. 30, N° 22, 2003.
- [5] Caires, S., A. Sterl and C. P. Gommenginger. C. P. Global Ocean Wave Period Data: Validation and Description. *J. Geophys. Res.*, Vol.110, c02003, doi:10.1029/2004JC002631, 2005.
- [6] Quilfen, Y., B. Chapron, B., F. Collard, and M. Serre. Calibration/validation of an altimeter wave period model and application to TOPEX/Poseidon and Jason Altimeters. *Marine Geodesy*, vol. 27, n° 3, 535 – 549, 2004.
- [7] Pontes, M.T. and Bruck, M., Using Remote Sensed Data for Wave Energy Resource Assessment, *Proc. 27th International Conference on Offshore Mechanics and Arctic Engineering (OMAE 2008)*, June 15-20, Estoril, Portugal, 2008.